FEASIBILITY STUDY ON USING FNA TO COMPLEMENT TNA IN LANDMINE DETECTION BY MONTE CARLO SIMULATION

Anan Sutcha[1], Chinorat Kobdaj[1] and Worasit Uchai[2*]

Received: Dec 8, 2011; Revised: May 23, 2012; Accepted: Jun 29, 2012

Abstract

MCNP5, a Monte Carlo computer code, is used to simulate the detection of TNT-landmines by using the technique of Fast Neutron Analysis (FNA) to complement Thermal Neutron Analysis (TNA). This technique utilizes a gamma ray detector to detect gamma rays induced from neutron interactions with the constituents of a TNT-landmine, H, C, O, and N, concurrently. The detection heads used in the simulation are composed of combinations of 2 isotopic neutron sources, ^{252}Cf and ^{241}Am-^{9}Be, and 3 gamma ray detectors, NaI, BGO, and $LaBr_3$. One kg of TNT, buried under 3 formation surfaces, sand, $CaCO_3$, and clay at 5 cm, is used as the dummy landmine. Flux ratios of 4 prominent gamma rays with energies of 2.22, 4.44, 6.13, and 10.83 MeV, which are induced from H, C, O, and N, respectively, are estimated and compared with their corresponding concentration ratios of the TNT-landmine's constituents. The estimated flux ratio between gamma rays induced from H and N based on using $LaBr_3$ to detect a TNT-landmine buried under sand agree with their corresponding concentration ratios between H and N within their error limits. However, the same ratios based on using other gamma ray detectors to detect a TNT-landmine buried under sand do not agree with their corresponding concentration ratios. Nevertheless, they are close, being less than 15% different. Other ratios of gamma ray fluxes induced from the TNT-landmine's constituents based on using other types of detection heads do not agree with their corresponding concentration ratios. These results imply that the complementary FNA-TNA technique cannot be used to detect a 1-kg TNT-landmine buried under a sand surface at 5 cm. However, the TNA technique which utilizes the detections of gamma rays induced from H and N concurrently should be able to detect such a landmine effectively.

Keywords: Monte Carlo simulation, TNT-landmine detection, fast neutron analysis, thermal neutron analysis

[1] *School of Physics, Institute of Science, Suranaree University of Technology, 111 University Avenue, Muang District, Nakhon Ratchasima, 30000, Thailand.*

[2] *Faculty of Liberal Arts and Science, Nakhon Phanom University, 176 Moo 8, Ban Nern Sa-ad, Naratchakhwai Sub District, Muang District, Nakhon Phanom 48200, Thailand. E-mail: uchai_col@hotmail.com*

[*] *Corresponding author*

Introduction

There are about 100 million abandoned landmines buried under ground in 70 countries around the world. These landmines cause serious humanitarian problems (Monin and Gillimore, 2002) because they either kill or maim people who accidentally step on them. It is believed that the numbers of people accidentally killed exceeds 25000 per year worldwide with even more maimed. The loss of life and injury create a tremendous burden on the governments of affected countries regarding the hospitalization of its maimed population. This problem is a consequence of a lack of efficient landmine detection equipment and methods. The existing equipment and methods which have been used for humanitarian demining (HD) are metal detectors, ground penetrating radar, sniffer dogs, and probing sticks. These equipment and these methods are insufficient for HD because they are too slow and expensive. There have been recommendations that nuclear techniques which utilize neutrons and gamma rays be used to produce more efficient equipment and methods (IAEA, 1999; 2001; 2003).

Nuclear Technique for Landmine Detection

There are various nuclear techniques used for landmine detection and one of the most promising techniques is the neutron-induced gamma ray technique. This technique relies on the detection of H, C, N, and O, the necessary elements of most landmines such as TNT ($C_7H_5N_3O_6$). H and C are fuel elements, O is the oxidizer, and N serves as a bonding agent that attaches itself to the elements of the molecule. An example of research work based on this technique is the Pulsed Elemental Analysis using Neutrons (PELAN) system (Vourvopoulos *et al.*, 2003). Recently, there have been 2 research works which involve using nuclear techniques to detect landmines. The first is the work of the Canadian Department of National Defense which developed a tele-operated, vehicle mounted, multi-sensor system to detect anti tank mines on roads and tracks in peacekeeping operations (Clifford *et al.*, 2007). Thermal Neutron Analysis (TNA) is the nuclear technique used in this work. Another one is the work of researchers at Bubble Technology Industries Inc., Chalk River, Ontario, Canada (Faust, 2004). Fast Neutron Analysis (FNA) in complement with TNA is used in this work. Since the interference due to gamma rays induced from fast neutron interactions with the constituents of ground formation is too high, the use of the complementary FNA-TNA technique for landmine detection is discouraged. However, the more comprehensive complementary FNA-TNA technique is used in this work to study whether it is feasible for landmine detection.

Complementary FNA-TNA Technique in Landmine Detection

For landmine detection with the complementary FNA-TNA technique, both fast and thermal neutron interactions are considered concurrently. The fast neutron interaction occurs when fast neutrons interact with C and O giving rise to the $^{12}C(n, n'\gamma)^{12}C$- and $^{16}O(n, n'\gamma)^{16}O$-inelastic collisions with subsequent emissions of the 4.44 and 6.13 MeV gamma rays, respectively. Analysis based on using these interactions is referred to as FNA. On the other side, fast neutrons can lose their energies through multiple collisions with the constituents of the ground formation and the landmine itself, becoming thermal neutrons with energies of 0.025 eV. These neutrons may be captured by H and N, giving rise to the $^{1}H(n, \gamma)^{2}H$- and $^{14}N(n, \gamma)^{15}N$-neutron capture interactions with the subsequent emissions of the 2.22 and 10.83 MeV gamma rays respectively. Analysis based on using these interactions is referred to as Thermal Neutron Analysis (TNA). The landmine detection technique based on using FNA and TNA concurrently is referred to as complementary FNA-TNA technique which considers the detections of 2.22, 4.44, 6.13, and 10.83 MeV gamma rays concurrently as its detection fingerprints

Scope of Work

In this work, a Monte Carlo computer code, MCNP5, is used to study the feasibility of using the complementary FNA-TNA technique in landmine detection by simulation. This computer code is a general-purpose particle transport program which uses a statistical process to simulate the transport of individual particles and record some aspects of their average behavior that can be inferred to be the average behaviors of the particles in a physical system. Due to limitation on this paper's space, details of MCNP5 are not given here but can be obtained from the MCNP manual (X-5 Monte Carlo Team, 2003). The landmine detection system used for simulation in this work comprises 3 types of detection heads and formations and a dummy landmine. A detection head is composed of a combination of 2 neutron sources, ^{252}Cf and ^{241}Am-^{9}Be, and 3gamma ray detectors, lanthanum bromide ($LaBr_3$: Ce), sodium iodide (NaI (Tl)) ,and bismuth germinate ($Bi_4Ge_3O_{12}$). The 3 types of formations used are dry sand (SiO_2), calcium carbonate ($CaCO_3$), and clay (a mixture of SiO_2, H and Al) with zero water content. TNT ($C_7H_5N_3O_6$) is used as the dummy landmine.

Geometry Model for Simulation

The geometry model of the landmine detection system used for simulation in this work has a cylindrical shape with dimensions as shown in Figure 1. In this model, the TNT-landmine with a density of 1.65 g/cm^3 is buried under sand, calcium carbonate, and clay formations with densities of 2.12, 2.71, and 2.6 g/cm^3, respectively. The position of the neutron source is at 5 cm directly under the gamma ray detector and 5 cm above the ground formation surface. ^{252}Cf emits neutrons in 2π directions downward to the landmine position with watt fission energy function of $f(E) = C\, exp(-E/a)\, sinh(bE)^{1/2}$, where a = 1.025 and b = 2.929, respectively. In the case of ^{241}Am-^{9}Be, the neutron energy distribution is taken from the graph of Figure 2 of Miri-Hakimabad *et al.* (2007) with the same direction as that of ^{252}Cf. All 3gamma ray detectors used have a diameter of 12.76 cm and the TNT-landmines buried under the ground formations at varying depths (0-20 cm) have varying masses (290, 500, 750, 1,000, 2000, and 3000 g). To reflect to the material types of the detectors, the ground formations, and the landmines used in the simulation, the same mass fractions of their materials' elements are as those given in Table 1 of Maučec and de Meijer (2002) and are entered as inputs in MCNP5.

Simulation Results

The combinations of the different types of detection systems constitute more than 100 simulation cases performed in this work. It is impossible to show every case of the simulation results and only those of some selected cases are shown here. These results are given in the form of the energy distribution of pulses (F-8 tally) created by radiation in association with the gamma ray detectors. Since, at high energies, the energy resolution of gamma ray detectors has little effect on the distribution of pulse height (Orion and Wielopolski, 2000), the response of the functions of all the gamma ray detectors used

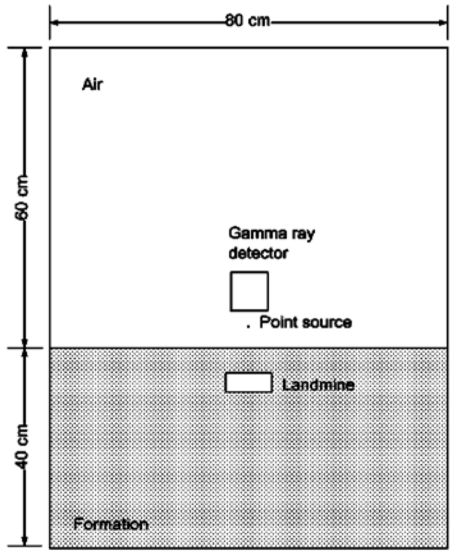

Figure 1. Geometry models for simulation

in this work are given in the same form: FWHM = a + b $\sqrt{E + cE^2}$, where a and c are approximately equal to 0 and b = 0.06 (Amgarou. *et al.*, 2009).

Simulation Results based on the Detection of TNT-landmine Buried under Sand

In this section, the simulation results based on the detection of a 1-kg TNT-landmine buried at 5 cm under sand are given. Though other lower TNT-masses are included in the simulation, their results are not shown here because the statistics of the 10.8 MeV gamma rays are not good. These results are based on using 6 different detection heads: ^{252}Cf/NaI, ^{241}Am-^{9}Be/NaI, ^{252}Cf/BGO, ^{241}Am-^{9}Be/BGO, ^{252}Cf/$LaBr_3$, and ^{241}Am-^{9}Be/$LaBr_3$. Figures 2(a) and 2(b) show the simulation results based on using ^{252}Cf/BGO- and ^{241}Am-^{9}Be/BGO- detection heads to detect the TNT-landmine buried under a sand surface at 5 cm, respectively. In both Figures, the top and bottom spectra represent the gamma ray spectra associated with using ^{252}Cf/BGO- and ^{241}Am-^{9}Be/BGO- detection heads to detect the TNT-landmine buried under the sand and on the surface of the sand, respectively. All 4 prominent gamma rays, which are the TNT-landmine detection fingerprints based on TNA and FNA, appeared on the spectra. They are the 2.22, 4.44, 6.13, and 10.83 MeV gamma rays, resulting from the ^{1}H(n, γ)^{2}H-, ^{12}C(n, n'γ)^{12}C-, ^{16}O(n, n'γ)^{16}O-, and ^{14}N(n, γ)^{15}N-reactions, respectively. Notice the appearances of gamma rays induced from the sand's constituents, the Si (n,γ)-2.23, O (n,α)-4.44, and O (n, n'γ)-6.13 MeV-gamma rays in the bottom spectra. Though the first 2 gamma rays seem not to give serious interferences with the TNT-landmine detection fingerprints because of

Table 1. Parameters used for calculation of concentration ratios of TNT's constituents (TNT's molecular formula: $C_7H_5O_6N_3$)

Energy (MeV)	Relative efficiency ($\in_i$)			σ_i(b)	f_i	A_i
	BGO	NaI(Tl)	$LaBr_3$:Ce			
H-2.22	1.00	1.00	1.00	0.33	0.62	5
C-4.44	0.92	0.98	0.67	0.18-0.43	0.72	7
N-10.83	0.54	0.96	0.34	0.11	0.79	3

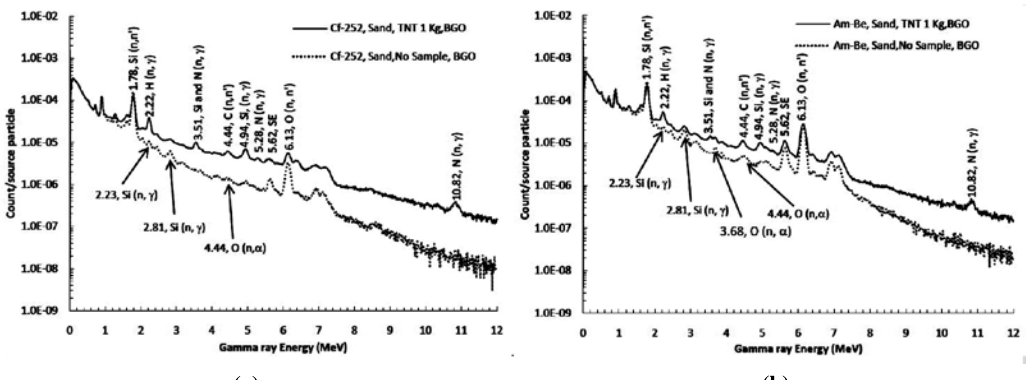

(a) (b)

Figure 2. Simulation results based on using ^{252}Cf/BGO- and ^{241}Am-^{9}Be/BGO- detection heads to detect TNT-landmine buried under sand surface at 5 cm

their low cross sections, the 6.13 MeV gamma rays do. The 6.13 MeV gamma rays definitely can not be used as a part of the landmine detection fingerprints because the majority of them are induced from oxygen, a constituent of sand.

Notice also the difference in the gaps between the Compton continuum of the top and bottom graphs of both Figures. Figure 2(b) shows a smaller gap than that of Figure 2(a). This effect is the result of the difference between the neutron energies of ^{241}Am-^{9}Be- and the ^{252}Cf-neutron sources; ^{241}Am-^{9}Be gives higher neutron energies than those of ^{252}Cf. Since higher neutron energy tends to induce more high energy gamma rays, ^{241}Am-^{9}Be tends to create higher gamma ray interferences. All these characteristics also appeared in the gamma ray spectra based on using ^{252}Cf/NaI-, ^{241}Am-^{9}Be/NaI-, ^{252}Cf/LaBr$_3$-, and ^{241}Am-^{9}Be/LaBr$_3$- detection heads. Due to the limits on this paper's space, the gamma ray spectra based on using these detection heads are not shown here.

Figure 3 shows comparisons between the gamma ray spectra induced from the detection of a 1-kg TNT-landmine buried under a sand surface at 5 cm based on using BGO-, NaI-, and LaBr$_3$- gamma ray detectors. Figure 3(a) and Figure 3(b) represent the gamma ray spectra based on using ^{252}Cf and ^{241}Am-^{9}Be as neutron sources, respectively. It is clear from both Figures that all 4 prominent gamma rays appeared on every spectrum. Spectra based on using BGO and LaBr$_3$ show the highest and lowest Compton continuums, respectively, while the NaI-spectrum shows the intermediate value. The Compton continuums of the gamma ray spectra based on using ^{241}Am-^{9}Be are higher than those using ^{252}Cf, as expected. These effects suggest that the ^{252}Cf/LaBr$_3$-detector head has an advantage over the other detection heads for TNT-landmine detection because it gives a gamma ray spectrum with less interference due to the lower Compton continuum.

Simulation Results of the Detection of TNT-landmine Buried under $CaCO_3$ and Clay

Figures 4(a) and 4(b) show the simulation results based on using ^{241}Am-^{9}Be/BGO-detection heads to detect a TNT-landmine buried under $CaCO_3$ and clayground formations, respectively. The top and bottom spectra represent results based on the detections of a TNT- landmine buried under the ground formations and on the surface of the groond, respectively. Their general characteristics are also similar to those spectra based on using sand as the ground formation. However, for the case of a TNT-landmine buried under $CaCO_3$, some low cross section gamma rays

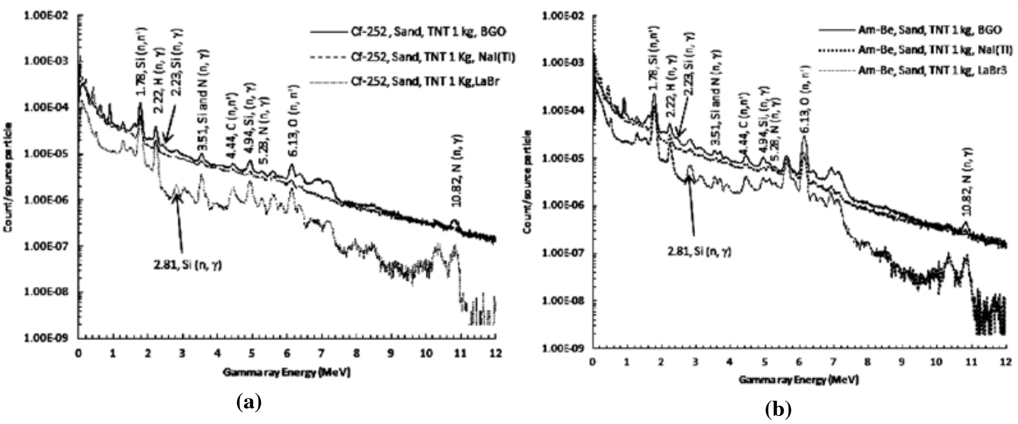

Figure 3. Simulation results based on using BGO-, NaI- and LaBr$_3$- gamma ray detectors to detect 1-kg of TNT-landmine buried under sand surface at 5 cm

(1.61, 1.91, 3.78, and 3.91 MeV) induced from neutron interactions with Ca, a constituent of $CaCO_3$, showed up. Though these gamma rays seem not to cause any interference, the 4.44 and 6.13 MeV gamma rays induced from C and O, 2 of the 4 constituents of $CaCO_3$, respectively, do. They have almost the same intensities as those induced from the TNT-landmine's constituents. These 2 gamma rays definitely cannot be used as parts of the fingerprints for TNT-landmine detection because they cause very high interferences. In the case of a TNT- landmine buried under clay, the 2.22 MeV gamma rays induced from the neutron interaction with H, a constituent of clay, may be an additional source of interference. Therefore, only the 10.83 MeV gamma rays induced from N may be used as a TNT-landmine detection fingerprint for this case

Discussion

In this section, ratios between the 2.22, 4.44, and 10.83 MeV gamma ray fluxes are estimated and compared with their corresponding concentration ratios of TNT's constituents. Since fluxes of these gamma rays are proportional to the number of nuclei of TNT's constituents, the ratios of these gamma ray fluxes should be equal to their corresponding concentration ratios of TNT's constituents. The next sections will discuss the derivation of the concentration ratios of TNT's constituents.

Derivation of Concentration Ratios of TNT's Constituents

Assuming that n_i is the number of nuclei of the ith constituent of TNT, the gamma ray flux induced from neutron interaction with the ith constituent, N_i, can be written as

$$N_i = \sigma_i \, n_i \qquad (1)$$

where σ_i is the cross section for producing the i^th gamma ray. The number of nuclei can be written as $n_i = \rho N_A A_i / M$, where ρ is the density of the TNT-landmine, N_A is the Avogadro's number (0.6022×10^{24} atoms/mol), A_i is the number of atoms of the i^th constituent of the TNT molecule, and M is the molecular weight of TNT. With the substitution of n_i into Equation (1), we obtain,

$$N_i = \sigma_i \frac{\rho N_A A_i}{M} \qquad (2)$$

Since these gamma rays are produced at the position of the TNT-landmine, they may not be detected by a gamma ray detector that is located at a distance away from the TNT-landmine. The gamma ray flux detected by a gamma ray detector can then be written as

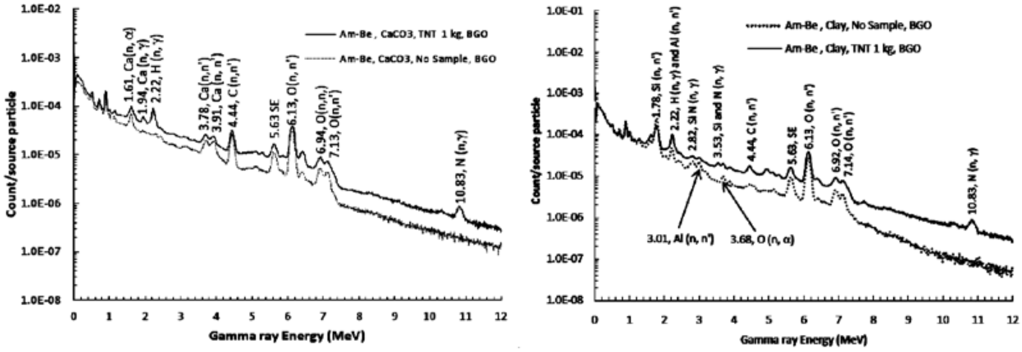

Figure 4. Simulation results based on using BGO to detect TNT-landmine buried under $CaCO_3$ and clay surfaces at 5 cm

$$C_i = N_i \in_i \Omega_d f_i \tag{3}$$

where $\in_i$, Ω_d, f_i are the relative efficiency of the detector, the detector's solid angle, and the gamma ray attenuation factor, respectively. The gamma ray attenuation factor in Equation (3) can be calculated from the expression $f_i = \exp(-(\mu/\rho)(\rho x))$. In this expression, μ and x are the gamma ray attenuation coefficient and the distance between the gamma ray detector and the TNT-landmine, respectively. With the substitution of Equation (2) in Equation (3), the gamma ray flux induced from the i[th] constituent of TNT can be written as

$$C_i = \sigma_i \in_i \Omega_d f_i \frac{\rho N_A A_i}{M} \tag{4}$$

By using Equation (4), the gamma ray fluxes of the induced prominent gamma rays can be estimated. The ratio between the 2.22 and 10.83 MeV gamma ray fluxes can, then, be written as

$$\frac{C_H}{C_N} = \frac{\sigma_H \in_H f_H A_H}{\sigma_N \in_N f_N A_N} \tag{5}$$

The ratios of other gamma ray fluxes, such as C_C/C_N and C_H/C_C, can be obtained in the same way. Since gamma rays induced from neutron interactions with TNT's constituents are proportional to the number of nuclei of TNT's constituents, the concentration ratios of TNT's constituents can be calculated by using Equation (5).

Table 2. Scaled photo peak net areas of the prominent gamma rays resulting from the detection of 1 kg TNT-landmine buried under sand surface at 5 cm

Energy	^{252}Cf			^{241}Am-^{9}Be		
	BGO	NaI(Tl)	$LaBr_3$:Ce	BGO	NaI(Tl)	$LaBr_3$:Ce
2.22	78255.00 ± 279.74	30211.00 ± 173.81	69958.00 ± 264.50	85446.00 ± 292.31	22760.00 ± 150.86	60868.00 ± 246.71
4.44	7460.00 ± 86.37	3319.00 ± 57.61	7689.00 ± 87.69	7460.00 ± 86.37	7522.00 ± 86.73	14437.00 ± 120.15
10.83	1274.00 ± 35.69	826.00 ± 28.74	623.00 ± 24.96	1404.00 ± 37.47	490.00 ± 22.14	528.00 ± 22.98

Table 3. Comparisons between calculated (theory) concentration ratios of TNT's constituents and simulated gamma ray flux ratios

Ratio	BGO			NaI(Tl)			$LaBr_3$:Ce		
	Theory	^{252}Cf	^{241}Am-^{9}Be	Theory	^{252}Cf	^{241}Am-^{9}Be	Theory	^{252}Cf	^{241}Am-^{9}Be
C_H/C_N	72.67	61.42 ± 1.73	60.86 ± 1.64	40.88	36.58 ± 1.29	46.45 ± 2.12	115.41	112.29 ± 4.52	115.28 ± 5.04
C_C/C_N	58.63	5.86 ± 0.18	5.31 ± 0.15	35.13	4.02 ± 0.16	15.35 ± 0.72	67.81	12.34 ± 0.36	27.34 ± 1.21
C_H/C_C	1.24	10.49 ± 0.13	11.45 ± 0.14	1.16	9.10 ± 0.17	3.03 ± 0.04	1.7	9.10 ± 1.74	4.22 ± 0.04

Comparisons between Gamma ray Flux Ratios and Concentration Ratios of TNT's Constituents

In this section, comparisons between the ratios of gamma ray fluxes resulting from the detection of the TNT-landmine buried under a sand surface at 5 cm and the concentration ratios of TNT's constituents are made. The ratio of gamma ray fluxes between the 2.22 and 10.83 MeV gamma rays can be obtained by taking the ratio of the scaled photo peak net areas of the simulated gamma ray spectra as shown in Table 2; (values are multiplied by the neutron source strength, 5 x 108 n/s). The corresponding concentration ratio (C_H/C_N) can be obtained by using Equation (5) and the parameters in Table 1.

As shown in Table 3, agreements between the simulated gamma ray flux ratios and the concentration ratios of TNT's constituents within their error limits are obtained in the C_H/C_N ratios based on using $^{252}Cf/LaBr_3$- and ^{241}Am-^{9}Be/ $LaBr_3$- detection heads. However, the C_H/C_N ratios based on using other detector heads do not agree with their corresponding concentration ratios, even though they are quite close (being less than 15% different). These results suggest that TNA can be used to detect a 1 kg TNT- landmine buried under sand at 5 cm effectively. Similar results are obtained for the case of a 1 kg TNT-landmine buried under $CaCO_3$, but they are different for the case of when it is buried under clay. Notice the large disagreements of the C_C/C_N and C_H/C_C ratios between the simulated gamma ray fluxes and the concentration of TNT's constituents in Table 3. These large disagreements are the results of the interferences at the 4.44 MeV gamma rays. The next section will discuss the possible sources of the interferences.

Possible Sources of Interference

Simulation results based on the detection of a single element is used to identify possible sources of interferences at the 2.22 and 4.44 MeV gamma rays. These results are in the form of a track length estimate (F-4 tally). Figures 5(a) and 5(b) show the simulated single element gamma ray spectra induced from the neutron interactions with the constituents of the TNT- landmine and the surface of the sabd (H, C, O, N, and Si) in the regions of 2.22 and 4.44 MeV. In Figure 5(a), it is obviously seen that the H-2.223 MeV gamma ray has slight interference from the 2.237 MeV gamma rays from Si (n,γ)- interactions because of their low cross section (0.003 b). However, there are 2 sources of interference at the 4.44 MeV due to the 4.439-MeV gamma rays from N (n,α)- and O(n,α)- interactions with cross sections of 0.036 and

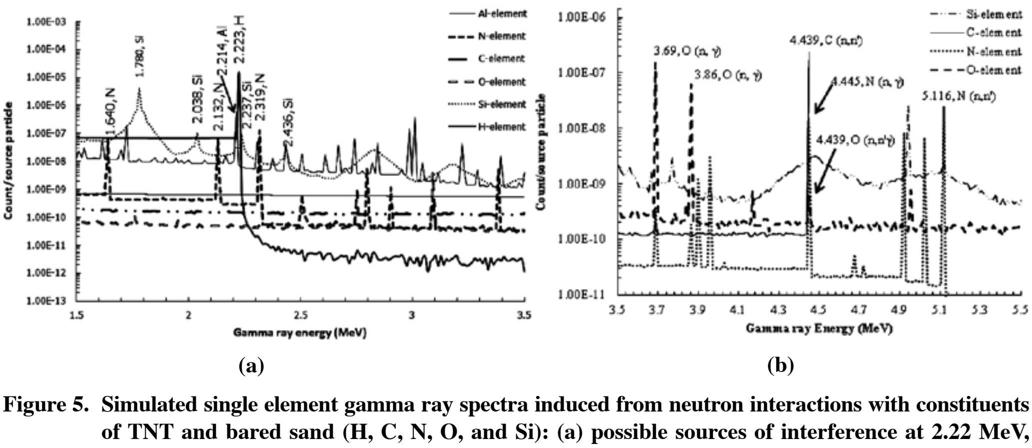

(a) (b)

Figure 5. Simulated single element gamma ray spectra induced from neutron interactions with constituents of TNT and bared sand (H, C, N, O, and Si): (a) possible sources of interference at 2.22 MeV, (b) possible sources of interferences at 4.44 MeV

0.014 b, respectively. Therefore, interferences at the 4.44 MeV could be very high. A similar interfering pattern occurred for the case of the TNT buried under $CaCO_3$. However, for the case of the TNT buried under clay, there is an additional high interference at the 2.22 MeV due to the Al (n, n'γ)-2.21 MeV gamma rays.

Conclusions

Due to intense interferences at 2 prominent gamma ray lines, the 4.44 and 6.13 MeV, the complementary FNA-TNA technique cannot be used to detect a 1kg TNT-landmine buried under a sand surface at 5 cm. This conclusion which agrees with the work of Faust, *et al.* (2004) is based on the disagreements of the C_C/C_N and C_H/C_C ratios between the simulated gamma ray flux ratios and their corresponding concentration ratios of the TNT's constituents. However, since the C_H/C_N ratios between the simulated gamma ray flux ratios and their corresponding concentration ratios, based on using $LaBr_3$, agree with each other within their error limits, the TNA technique based on the detections of the H-2.22 and N-10.83 MeV gamma ray, concurrently, should be able to detect a 1 kg TNT-landmine buried under a sand surface at 5 cm efficiently. For the case of such a TNT-landmine buried under $CaCO_3$ at 5 cm, similar results as for that buried under sand are obtained. Therefore, the TNA technique based on the detections of 2.22 and 10.83 MeV gamma rays, concurrently, should be able to detect a 1 kg TNT-landmine buried under sand and $CaCO_3$, effectively. However, for the case of such a TNT-landmine buried under clay, there is high interference at the 2.22 MeV due to the Al (n, n'γ)-2.21 MeV gamma rays with a cross section of 0.118 b. The TNA technique must depend on the detection of the 10.83 MeV gamma rays alone for this case. The simulation results in this work suggest that, for the TNA-based landmine detection, ^{252}Cf gives better results than those of ^{241}Am-^{9}Be because ^{252}Cf gives less gamma ray interference. Furthermore, the simulation results show that a TNT- landmine is itself a good neutron moderator giving higher moderating power for the higher mass of a TNT-landmine. This result, which agrees with the result from the work of Brooks *et al.* (2004), is reasonable because TNT has a high percentage of H as its content.

Suggestion

The TNA technique should be used to experimentally test the results of this work. It is almost impossible to use the complementary FNA-TNA technique in TNT- landmine detection because of the high interferences by gamma rays induced from the ground formation's constituents.

References

Amgarou, K., Domingo, C.T., Bouassoule, T., and Fernandez, F. (2009). Monte Carlo simulation of the NaI(Tl) detector response to measure gold activated foils. Nucl. Instrum. Meth. B., 267:2944–2951.

Brooks, F.D., Drosg, M., Buffler, A., and Allie, M.S. (2004). Detection of anti-personnel landmines by neutron scattering and attenuation. Appl. Radiat. Isotopes, 61:27-34

Clifford, E.T.H., McFee, J.E., Ing, H., Andrews, H.R., Tennant, D., Harper, E., and Faust, A.A. (2007). A militarily fielded thermal neutron activation sensor for landmine detection. Nucl. Instrum. Meth. A., 579:418-425

Faust, A.A. (2004). Feasibility of Fast Neutron Analysis (FNA) for Detection of Buried Landmines. Final report BTI-04/60-30. Bubble Technology Industries Inc.,Chalk River, ON, Canada.

IAEA. (1999). Proceedings of the First Research Coordination Meeting on the Application of Nuclear Techniques to Anti-personnel Landmines Identification; November 23-26,1999; Zagreb, Croatia. IAEA/PS/RC-799.

IAEA. (2001). Proceedings of the Second Research Coordination Meeting on the Application of Nuclear Techniques to Anti-personnel Landmines Identification; September 11-14, 2001; St Petersburg, Russia. IAEA/PS/RC-799-2.

IAEA. (2003). Proceedings of the Final Research Coordination Meeting on the Application of Nuclear Techniques to Anti-personnel Landmines Identifiation; May 19-23, 2003; Vienna, Austria.

Maućec, M..and de Meijer, R. J. (2002). Monte Carlo simulations as a feasibility tool for non-metallic land-mine detection by thermal-neutron backscattering. Appl. Radiat. Isotopes, 56:837-846

Miri-Hakimabad, H., Vejdani-Noghreiyan, A., and Panjeh, H. (2007). Improving the moderator geometry of an anti-personnel landmine detection system. Appl. Radiat. Isotopess, 66:606-611.

Monin, L. and Gallimore, A. (2002). The Devil's Gardens: A History of Landmines. Pimlico Books, London, 234 p.

Orion, I. and Wielopolski, L. (2000). Response Function of the BGO and NaI(T1) Detectors Using Monte Carlo Simulation. Ann.NY Acad. Sci., 904:271-275.

Vourvopoulos, G., Sullivan, R.A., Knapp, V., and Hrupec, D. (2003). Evaluation of PELAN as confirmation sensor. In: EUDEM2-SCOT-2003, International Conference on Requirements and Technologies for the Detection, Removal and Neutralization of Landmines and UXO. Sahli, H., Bottoms, A.M., and Cornelis, J. (eds.), September 15-18,2003; Vrije Universiteit, Brussels, Belgium. p. 731-736.

X-5 Monte Carlo Team. (2003). MCNP-A General Monte Carlo N-Particle Trans-port Code., Version5, Technical Report, Los Alamos National Lab-oratory, Los Alamos, NM, USA.